



HAL
open science

Effects of the anthelmintic drug PF1022A on mammalian tissue and cells

R. Dornetshuber, M.R. Kamyar, P. Rawnduzi, I. Baburin, K. Kouri, E. Pilz, T. Hornbogen, R. Zocher, W. Berger, R. Lemmens-Gruber

► **To cite this version:**

R. Dornetshuber, M.R. Kamyar, P. Rawnduzi, I. Baburin, K. Kouri, et al.. Effects of the anthelmintic drug PF1022A on mammalian tissue and cells. *Biochemical Pharmacology*, 2009, 77 (8), pp.1437. 10.1016/j.bcp.2009.01.005 . hal-00493486

HAL Id: hal-00493486

<https://hal.science/hal-00493486>

Submitted on 19 Jun 2010

HAL is a multi-disciplinary open access archive for the deposit and dissemination of scientific research documents, whether they are published or not. The documents may come from teaching and research institutions in France or abroad, or from public or private research centers.

L'archive ouverte pluridisciplinaire **HAL**, est destinée au dépôt et à la diffusion de documents scientifiques de niveau recherche, publiés ou non, émanant des établissements d'enseignement et de recherche français ou étrangers, des laboratoires publics ou privés.

Accepted Manuscript

Title: Effects of the anthelmintic drug PF1022A on mammalian tissue and cells

Authors: R. Dornetshuber, M.R. Kamyar, P. Rawnduzi, I. Baburin, K. Kouri, E. Pilz, T. Hornbogen, R. Zocher, W. Berger, R. Lemmens-Gruber



PII: S0006-2952(09)00025-2
DOI: doi:10.1016/j.bcp.2009.01.005
Reference: BCP 10064

To appear in: *BCP*

Received date: 28-11-2008
Revised date: 7-1-2009
Accepted date: 8-1-2009

Please cite this article as: Dornetshuber R, Kamyar MR, Rawnduzi P, Baburin I, Kouri K, Pilz E, Hornbogen T, Zocher R, Berger W, Lemmens-Gruber R, Effects of the anthelmintic drug PF1022A on mammalian tissue and cells, *Biochemical Pharmacology* (2008), doi:10.1016/j.bcp.2009.01.005

This is a PDF file of an unedited manuscript that has been accepted for publication. As a service to our customers we are providing this early version of the manuscript. The manuscript will undergo copyediting, typesetting, and review of the resulting proof before it is published in its final form. Please note that during the production process errors may be discovered which could affect the content, and all legal disclaimers that apply to the journal pertain.

Effects of the anthelmintic drug PF1022A on mammalian tissue and cells

R. Dornetshuber^{1,2}, M.R. Kamyar¹, P. Rawnduzi¹, I. Baburin¹, K. Kouri¹, Pilz E.¹, T.

Hornbogen³, R. Zoher³, W. Berger², R. Lemmens-Gruber¹

¹Department of Pharmacology and Toxicology, University of Vienna, Althanstr. 14, A-1090

Vienna, Austria

² Institute of Cancer Research, Department of Medicine I, Borschkegasse 8a, Medical

University of Vienna, 1090 Vienna, Austria.

³ Technical University of Berlin, Franklinstr. 29, D-10587 Berlin, Germany

Corresponding author:

Rosa Lemmens-Gruber

Department of Pharmacology and Toxicology, University of Vienna

Althanstr. 14

A-1090 Vienna

Austria

rosa.lemmens@univie.ac.at

Tel. +43-1-4277-55325

FAX +43-1-4277-9553

Keywords:

PF1022A, anthelmintics, ionophore, cytotoxicity, apoptosis

Abstract

1
2
3 Nematode infections cause human morbidity and enormous economic loss in livestock. Since
4
5 resistance against currently available anthelmintics is a worldwide problem, there is a
6
7 continuous need for new compounds. The cyclooctadepsipeptide PF1022A is a novel
8
9 anthelmintic that binds to the latrophilin-like transmembrane receptor important for
10
11 pharyngeal pumping in nematodes. Furthermore, PF1022A binds to GABA receptors, which
12
13 might contribute to the anthelmintic effect. Like other cyclodepsipeptides, PF1022A acts as
14
15 an ionophore. However, no correlation between ionophoric activity and anthelmintic
16
17 properties was found. This is the first study describing the effect of PF1022A on mammalian
18
19 cells and tissues. While channel-forming activity was observed already at very low
20
21 concentrations, changes in intracellular ion concentrations and reduction of contractility in
22
23 isolated guinea-pig ileum occurred at multiples of anthelmintically active concentrations.
24
25 PF1022A did not induce necrotic cell death indicated by complete lack of cellular lactate
26
27 dehydrogenase release. In contrast, apoptosis induction via the mitochondrial pathway was
28
29 suggested for long-term drug treatment at high concentrations due to numerous apoptotic
30
31 morphological changes as well as mitochondrial membrane depolarisation. Short time effects
32
33 were based on cell cycle blockade in G₀/G₁ phase. Additionally, the cell cycle and apoptosis
34
35 regulating proteins p53, p21 and bax, but not Bcl-2 were shown to impact on PF1022A-
36
37 induced cytotoxicity. However, since PF1022A-induced cytotoxicity was found at drug
38
39 concentrations higher than those used in anthelmintic treatment, it can be suggested that
40
41 PF1022A intake might not impair human or animal health. Thus, PF1022A seems to be a safe
42
43 alternative to other anthelmintic drugs.
44
45
46
47
48
49
50
51
52
53
54
55
56
57
58
59
60
61
62
63
64
65

1. Introduction

1
2
3 Nematode infections are a major cause of human morbidity and mortality in tropic and
4
5 temperate climates [1]. Moreover, these pathogens cause enormous economic loss in cattle,
6
7 horses, pigs and sheep [2, 3]. However, resistance against the major currently available
8
9 anthelmintics has increasingly become a worldwide problem [4]. Therefore, new compounds
10
11 with different modes of action are needed to manage the problem of resistance. The 24-
12
13 membered N-methylated cyclooctadepsipeptide PF1022A belongs to a novel class of
14
15 anthelmintic agents with potent broadspectrum anthelmintic activity and low toxicity in
16
17 animals [5, 6, 7, 8, 9]. Additionally this drug was found to be a good candidate for the
18
19 treatment of human angiostrongyliasis [10].
20
21

22
23
24 PF1022A is a secondary metabolite of the fungus imperfectus *Mycelia sterilia* (*Rosellinia* sp.)
25
26 isolated from the plant *Camellia japonica* [5]. So far, the nonribosomal N-methyl-
27
28 cyclooctadepsipeptide synthetase responsible for PF1022A biosynthesis has been isolated and
29
30 characterized [11]. Consequently, this discovery allows the development of new N-methyl-
31
32 cyclooctadepsipeptide-derived compounds [12]. PF1022A serves as starting material for the
33
34 synthesis of semi-synthetic cyclooctadepsipeptide derivatives with improved anthelmintic
35
36 potency and broadspectrum activity [13, 14, 15, 16]. Meanwhile, also total synthesis of
37
38 cyclooctadepsipeptides has been accomplished [17, 18, 19, 20, 21, 22].
39
40
41

42
43
44 With regard to the molecular mechanisms underlying its anthelmintic activity, PF1022A has
45
46 been shown to bind to the amine terminus of the 110-kDa heptahelical, latrophilin-like
47
48 transmembrane receptor HC-110R, isolated from *Haemonchus contortus* (Rudolphi). This
49
50 receptor has an important regulatory function on pharyngeal pumping in nematodes. By
51
52 binding to this receptor, PF1022A induces an influx of external Ca^{2+} into the cell [23],
53
54 consequently affecting several presynaptic signal transduction pathways [24]. Due to this
55
56 effect, treatment with PF1022A as well as the semi-synthetic emodepside causes worm
57
58
59
60
61
62
63
64
65

1
2
3
4
5
6
7
8
9
10
11
12
13
14
15
16
17
18
19
20
21
22
23
24
25
26
27
28
29
30
31
32
33
34
35
36
37
38
39
40
41
42
43
44
45
46
47
48
49
50
51
52
53
54
55
56
57
58
59
60
61
62
63
64
65

paralysis [24, 25]. These modes of action are different from the mechanisms of known anthelmintics like benzimidazoles, imidazothiazoles, tetrahydropyrimidines and macrocyclic lactones [26]. Thus, these new drugs might solve the increasing problem of resistance development against available anthelmintics. Indeed, PF1022A and emodepside were effective in benzimidazole-, levamisole- and ivermectin-resistant populations of *Haemonchus contortus* in sheep when applied orally, subcutaneously or intravenously. Additionally, they showed activity in ivermectin-resistant *Cooperia oncophora* population in cattle [3].

Furthermore, in binding studies it could be demonstrated that PF1022A binds to GABA receptors in nematodes, which might contribute to the anthelmintic effect [27]. PF1022A acts as an ionophore in planar lipid bilayers like other cyclodepsipeptides, however, testing structurally related derivatives revealed no correlation between ionophoric activity and anthelmintic properties [28].

However, at least to our knowledge, no data describing the effect of PF1022A on mammalian cells and tissues are published so far. PF1022A is structurally related to cyclohexadepsipeptides of the enniatin-type for which synergistic effects on antifungal drug activity were described [29, 30]. Moreover, potent cytostatic and cytotoxic effects against diverse cancer cell types [31, 32, 33], antiangiogenic activity [34] as well as anthelmintic properties [35] could be demonstrated for these structurally related cyclohexadepsipeptides.

Aim of this study was to investigate the effect of PF1022A on force of contraction in isolated guinea-pig ileum, its electrophysiological properties and the resulting impacts on cell homeostasis. Moreover, PF1022A-induced cytotoxic modes of action were elucidated in mammalian cells.

2. Materials and Methods

2.1. Test compound

PF1022A was kindly supplied by Bayer AG, Germany. The compound is poorly soluble in water, therefore a stock solution with Tween 80 : MeOH = 1:2 (Sigma-Aldrich, Vienna, Austria) was prepared. This solution was further diluted to the nutrient solution at the final concentration.

2.2. Cell lines

The following human cell lines were used in this study: the epidermal carcinoma-derived cell line KB-3-1 (generously donated by Dr. Shen, Bethesda, USA) [36], and the colon carcinoma cell line CaCo-2 (American Tissue Culture Collection), the colon carcinoma cell model HCT116 and respective sublines with deleted p53, p21, or bax genes were generously donated by Dr. Vogelstein, John Hopkins University, Baltimore [37, 38, 39], and the Bcl-2-negative non-small cell lung cancer cell line A549 and its bcl-2 pBabe/Puro-transfected subline [31]. HCT116 cell lines were grown in McCoy's culture medium, Caco-2 cells in MEME, and KB-3-1 as well as A549 cells and the transfected subline in RPMI 1640 medium. All culture media were purchased from Sigma-Aldrich GmbH (St. Louis, MO) and supplemented with 10% fetal calf serum (PAA, Linz, Austria). Cultures were periodically checked for *Mycoplasma* contamination.

2.3. Contractility measurement

The effect of PF1022A on force of contraction (f_c) of isolated terminal ilea of the guinea pig was studied as previously described [40]. All chemicals were purchased by Sigma-Aldrich

(Vienna, Austria). The test compound was added cumulatively to the bathing solution in rising concentrations every 30 min when a steady-state effect has been reached.

2.4. Ionophoric activity – single channel current

Electrical activity was studied on CaCo-2 cells at room temperature (19-22°C) as previously described [40, 48]. Chemicals for pipette and bathing solutions were supplied by Sigma-Aldrich (Vienna, Austria). After a control period of 15 min during which no electrical activity could be observed, PF1022A was added to the bathing solution. The wash-in phase lasted about 1 to 2 min until single channel current could be detected. The same experimental protocol ($E_h = -60, -40, -20, 0, +20, +40, +60$ mV) was applied as during control recordings. Electrophysiological measurements were carried out with an Axopatch-1D patch clamp amplifier (Axon Instruments, CA) at a cut-off frequency (-3 dB) of 2 kHz. Currents were filtered at 5 kHz with a dual variable filter (VBF 8, Kemo Ltd, Beckenham, Kent, U.K.), digitized via an AD converter (TL-1 interface, Axon Instruments, CA) and sampled at 5-10 kHz. Data acquisition and storage were processed directly to a PC equipped with pCLAMP 6 software (Axon Instruments, CA). Single channel analysis was performed with the ASCD software (G. Droogmans, Leuven, Belgium).

2.5. Two-microelectrode voltage clamp studies - GABA_A receptor

Stage V-VI oocytes from *Xenopus laevis* were prepared and cRNA injected as previously described [41, 42]. On the 2nd day after cRNA injection, electrophysiological experiments were performed by the two-microelectrode voltage clamp method using of a TURBO TEC 01C amplifier (npi electronic GmbH, Tamm, Germany) at a holding potential of -70 mV. The bath solution contained 90 mM NaCl, 1 mM KCl, 1 mM MgCl₂, 1 mM CaCl₂ and 5 mM HEPES (pH 7.4). PF1022A was co-applied with GABA EC₃₋₁₀ (effective concentration of

1 GABA that induces 3-10 % of maximal GABA-evoked current) by means of an automated
2 fast perfusion system according to [43]. Percent potentiation of I_{GABA} by the PF1022A was
3
4 calculated using formula: $(R/C)*100\%$, where R is the amplitude of the chloride current
5 evoked by co-application of control GABA EC₃₋₁₀ and the indicated concentration of the
6
7 compound, and C is the amplitude of the chloride current evoked by application of control
8
9 GABA EC₃₋₁₀ alone.
10
11
12
13

14 **2.6. Fluorescence imaging**

15
16
17 Caco-2 cells were loaded with 1 μM FURA 2AM and an equivalent concentration of Pluronic
18
19 20% in DMSO at room temperature (18-23°C) for 30-45 min. Fluorescent dye and Pluronic
20
21 were procured from Molecular Probes (Leiden, The Netherlands). After washout cells were
22
23 allowed to hydrolyze the dye for 30 minutes to one hour, and experiments were performed as
24
25 previously described [47]. Ratiometric measurements were realized following background
26
27 subtraction with the Axon Imaging Workbench 2.2 software (Axon Instruments, CA)
28
29 averaging 2 frames. Results are presented as the relative change $(-\Delta F/F_0)$ of the F_{340}/F_{380}
30
31 signal.
32
33
34
35
36
37
38
39
40

41 **2.7. Cell viability assays**

42
43 KB-3-1 cells were seeded (2×10^4 cells/ml) in 96-well plates and were allowed to recover for
44
45 24 h. Concentrations of PF1022A ranging from 0.5 μM up to 10 μM were applied with an
46
47 incubation time of 24, 48 and 72 h. The cytotoxic effect of PF1022A was determined with an
48
49 MTT-based vitality assay (EZ4U, Biomedica, Vienna, Austria) as described previously [31].
50
51 Moreover, to study the reversibility of the cytotoxic PF1022A effect, after an incubation time
52
53 of 1, 2, 4, 6, 8, 24 and 48 h the test compound was removed from the wells and substituted by
54
55
56
57
58
59
60
61
62
63
64
65

1 fresh medium. After a total incubation period of 72 h the EZ4U assay was performed and data
2 were evaluated by means using the GraphPadPrism 4 software.
3
4

5 6 7 **2.8. Lactate dehydrogenase release assay**

8
9 The release of lactate dehydrogenase (LDH) from the cytosol, which indicates loss of
10 membrane integrity and is further associated with necrotic cell death, was studied with a
11 cytotoxicity detection kit (Roche, Basel, Switzerland). Adherent KB-3-1 cells (2×10^4 cells/ml)
12 were incubated in 96-well plates for 24 h with PF1022A (0.5 μ M - 10 μ M). Afterwards, from
13 each well 100 μ l of the supernatant was transferred to a 96-well microplate and incubated for
14 20 min at 37°C with reagent solution of the kit according to the manual. Finally, absorbance
15 was measured with a microplate reader, set at 490 nm and 620 nm as reference.
16
17
18
19
20
21
22
23
24
25
26
27

28 29 **2.9. DAPI Staining**

30
31 1×10^5 KB-3-1 cells/well were treated in 6 well plates with 2.5 – 10 μ M PF1022A for 24 h and
32 48 h, respectively. Subsequently, cells were harvested, cytopins were prepared, and apoptosis
33 was evaluated by staining with 4',6-diamidino-2-phenylindole (DAPI) containing antifade
34 solution (Vector Laboratories, Inc., Burlingame, CA). The nuclear morphology of cells was
35 examined with a Leica DMRXA fluorescence microscope (Leica Mikroskopie and System,
36 Wetzlar, Germany) equipped with appropriate epifluorescence filters and a COHU charge-
37 coupled device camera. The rate of apoptosis was determined as the percentage of apoptotic
38 nuclei of at least 500 nuclei/experimental group.
39
40
41
42
43
44
45
46
47
48
49
50
51
52

53 54 **2.10. Cell cycle analysis**

55
56 Adherent KB-3-1 (5×10^5 cells/well) were incubated in 6-well plates at 37°C for 24 or 48 h
57 with 0.5, 1, 2.5, 5 and 10 μ M PF1022A. Cell cycle progression was analysed by flow
58
59
60
61
62
63
64
65

1 cytometry using FACS Calibur (Becton Dickinson, Palo Alto CA) as described [44]. Cell
2 Quest Pro software (Becton Dickinson and Company, New York, USA) was used to analyse
3 the resulting DNA histograms.
4
5
6
7
8

9 **2.10. Detection of mitochondrial membrane potential**

10 KB-3-1 cells (5×10^6 cells/well) were exposed to 1, 2.5, 5 and 10 μM PF1022A for 24 h before
11 cell staining was performed with the fluorescent dye 5,5',6,6'-tetrachloro-1,1',3,3'-tetraethyl-
12 benzimidazolylcarbocyanine iodide (JC-1; Mitochondrial Membrane Potential detection Kit;
13 Stratagene, La Jolla, CA, USA) as described [31, 44].
14
15
16
17
18
19
20
21
22
23

24 **2.11. Statistical analysis**

25 Values are expressed as means \pm S.E. where appropriate. Significance was calculated with
26 Student's t-test for paired (f_c) and unpaired observations. Statistical significance was
27 determined at levels of $P < 0.05$, $P < 0.01$ and $P < 0.001$.
28
29
30
31
32
33
34
35
36
37
38

39 **3. Results**

40 **3.1. Effect on force of contraction**

41 Isometrically measured f_c of isolated, pre-contracted (60 mM KCl) terminal ilea of the guinea
42 pig was concentration-dependently (0.1 to 30 μM PF1022A) decreased with an IC_{50} of 25 ± 3
43 μM ($n=3$). At solvent concentrations up to 3.5 μl methanol/Tween in 28 ml nutrient solution,
44 which corresponds to the solvent concentration at 10 μM PF1022A, no effect on contractility
45 of isolated smooth muscle preparations was observed. At 10 μl methanol/Tween in 28 ml
46 nutrient solution, that is the solvent concentration at 30 μM PF1022A, f_c was decreased by
47
48
49
50
51
52
53
54
55
56
57
58
59
60
61
62
63
64
65

1
2
3
4
5
6
7
8
9
10
11
12
13
14
15
16
17
18
19
20
21
22
23
24
25
26
27
28
29
30
31
32
33
34
35
36
37
38
39
40
41
42
43
44
45
46
47
48
49
50
51
52
53
54
55
56
57
58
59
60
61
62
63
64
65

4.4% (n=3). Therefore, results obtained with 30 μM PF1022A were corrected for this solvent induced decrease in contractility. Reduction of f_c was only significant at 30 μM PF1022A (n=3, $P < 0.05$). At the anthelmintically active concentration of 1 μM PF1022A [6], the decrease of f_c from the control value of 17.8 ± 2.6 mN to 15.9 ± 2.2 mN was not significant (n=3, $P > 0.05$).

3.2. Pore-forming activity

After a control period of 15 min during which no electrical activity could be observed at holding potentials between -60 and $+60$ mV, PF1022A was added to the bathing solution. One to two minutes after addition of 1 μM PF1022A pore forming activity was detected in inside-out patches of Caco-2 cells with mono- and divalent cations (Na^+ , K^+ , Ca^{2+}) as the charge carriers. Higher PF1022A concentrations achieved similar effects, but faster onset of action and multiple channel openings (Fig. 1A). Washout of the substance was not effective indicating permanent incorporation into the cell membrane.

The experimental reversal potentials for potassium (n=3) and sodium (n=3) were comparable to the theoretical values for the ionic equilibrium potential calculated according to the Nernst equation. Further, current amplitudes did not vary when aspartate was substituted by chloride in the K^+ and Na^+ bathing solutions in equal cation molarity (n=3), also indicating the channel's cationic selectivity.

Current to voltage relationships for potassium, sodium and calcium currents presented a symmetrical behaviour upon hyper- and depolarization, rectifying at potentials higher than -20 mV and $+20$ mV. Single channel conductance was therefore estimated in the linear range of -20 mV to $+20$ mV and was calculated for K^+ at 39.3 ± 2.8 pS (n=5), for Na^+ at 52.3 ± 3.0 pS (n=5) and for Ca^{2+} at 50.5 ± 2.2 pS (n=3).

1
2
3
4
5
6
7
8
9
10
11
12
13
14
15
16
17
18
19
20
21
22
23
24
25
26
27
28
29
30
31
32
33
34
35
36
37
38
39
40
41
42
43
44
45
46
47
48
49
50
51
52
53
54
55
56
57
58
59
60
61
62
63
64
65

Probability density functions for open times of the PF1022A channel conducting potassium, sodium or calcium ions at potentials ranging from -60 to +60 mV could be fitted with one exponential. The kinetics of the openings at those potentials was not significantly ($P>0.05$) affected by voltage. Further, time constants for open times did not significantly differ for Na^+ , K^+ and Ca^{2+} ($P>0.05$). Open state probability was independent of voltage, however, varying markedly in different patches and also within one patch with time. Openings occurred usually in bursts of fast flickerings, which alternated with periods of electrical inactivity. For Ca^{2+} conducting channels these periods without electrical activity were almost twice the duration of those with the studied monovalent cations.

3.3. Effect on intracellular ion concentration

For studying the effect of PF1022A on intracellular calcium, sodium and potassium concentrations, the ionophores ionomycin, gramicidine and valinomycin ($n=3$ for each) were used as reference compounds. Although PF1022A incorporated into the cell membrane leading to conduction of calcium, sodium and potassium ions, for Na^+ ions no effect on the intracellular concentration was observed, while the intracellular K^+ and Ca^{2+} concentrations were changed. The effect of PF1022A on intracellular Ca^{2+} concentration, however, was weak compared to the control with ionomycin. Representative recordings are presented for Ca^{2+} in Figure 1B and C. Only a small increase in the intracellular Ca^{2+} concentration was caused by 100 μM PF1022A ($n=7$) compared to 100 μM ionomycin, while at 10 μM PF1022A (a concentration causing multiple channel openings, see Fig. 1A, $n=6$) no changes in $[\text{Ca}^{2+}]_i$ were observed (data not shown). The effect on intracellular K^+ concentration is illustrated for 100 μM PF1022A (E) and 100 μM valinomycin (D) for two representative cells each. The effect on intracellular K^+ was more pronounced than on intracellular Ca^{2+} , but still weak at

1 concentrations that already caused multiple channel openings (10 μ M, n=6), and ineffective at
2 1 μ M PF1022A (n=5).
3
4
5
6

7 **3.4. Effect on chloride currents through GABA_A receptors by PF1022A**

8

9 As an anthelmintic effect via binding to the GABA receptor in nematodes was suggested [27],
10 we also studied the electrophysiological effect of PF1022A on GABA_A channels. An effect on
11 this channel is of interest e.g. in respect to sedative side effects of the drug. At 1 and 10 μ M
12 PF1022A, the potentiation of GABA-activated chloride current (I_{GABA}) through $\alpha 1\beta 2\gamma 2S$
13 receptors was $20.8 \pm 11.2\%$ (n=4) and $78.2 \pm 16.1\%$ (n=6), respectively. However, an effect of
14 PF1022A on GABA_A can be excluded, because the solvent-induced increase in I_{GABA} was
15 $70.8 \pm 39.4\%$ at a solvent concentration which corresponds to the concentration present at 10
16 μ M PF1022A.
17
18
19
20
21
22
23
24
25
26
27
28
29
30

31 **3.5. Effects of PF1022A on cell proliferation and viability**

32

33 To investigate the impact of the anthelmintic drug PF1022A on human cell proliferation,
34 dose-response curves (0.5-10 μ M) were established in human KB-3-1 cells using different
35 exposure times. Based on MTT assays an increased cell proliferation was observed in KB-3-1
36 cells after 24 and 48 h exposure to PF1022A concentrations ≤ 1 μ M (Fig. 2). The maximal
37 increase in cell growth (1.25-fold) was observed after 24 h incubation with 0.5 μ M PF1022A.
38 At higher PF1022A concentrations the number of viable cells decreased concentration
39 dependently with an IC_{50} of 8.1 μ M (24 h), 6.6 μ M (48 h) and 5.9 μ M (72 h), respectively.
40 Moreover, recovery of cells exposed for 1, 2, 4, 6, 8, 24 or 48 h to increasing PF1022A
41 concentrations was studied after 72 h. These experiments revealed enhanced cell proliferation
42 at concentrations ≤ 2.5 μ M and short exposure times (1 to 8 h). A maximum growth
43 stimulation (1.3-fold growth) was obvious at 2 h treatment with 2.5 μ M PF1022A. However,
44
45
46
47
48
49
50
51
52
53
54
55
56
57
58
59
60
61
62
63
64
65

1 in experiments with expanded drug exposure time (24 and 48 h), no stimulating effect was
2 observed (data not shown). This is in contrast to experiments without wash-out phase (Fig. 2).
3
4 The cytotoxic effect at higher drug concentrations ($>5 \mu\text{M}$) and long time exposure (24 and
5 48 h) did not differ significantly from data obtained without wash-out. This indicates potent
6 cytotoxic effects of PF1022A at high concentrations (data not shown).
7
8
9
10

11 **3.6. Apoptosis induction by PF1022A**

12 To gain more insights into the PF1022A-induced cell death, LDH release from mitochondria
13 to cytosol, which is indicative for necrotic cell death, was measured. Since no cytosolic LDH
14 was detectable after 24 h PF1022A treatment at concentrations ranging from 0.5-10 μM (data
15 not shown), we hypothesized that the decrease in the number of viable cells was due to
16 apoptotic cell death. This was further confirmed by results obtained by Dapi stainings of
17 control and PF1022A-treated KB-3-1 cells. By direct counting under the microscope a
18 concentration- and time-dependent increase of apoptotic nuclei was observed indicated by
19 characteristic apoptotic features like cell shrinkage, chromatin condensation and apoptotic
20 body formation. In more detail, after 24 h exposure to 2.5, 5 and 10 μM PF1022A a relative
21 minor increase in the number of apoptotic nuclei from 2% in the control to 4%, 12% and 14%
22 was observed (Fig. 3A). In contrast, after 48 h treatment with the above mentioned PF1022A
23 concentrations the proportion of apoptotic nuclei remarkably increased from 3% in the control
24 to 6%, 15% and 36%, respectively (Fig. 3B).
25
26
27
28
29
30
31
32
33
34
35
36
37
38
39
40
41
42
43
44
45
46
47

48 Since programmed cell death can be initiated via the so-called mitochondrial pathway which
49 is based on depolarisation of the outer mitochondrial membrane, FACS analyses with JC-1-
50 stained KB-3-1 cells were performed. JC-1 is a lipophilic cation fluorescent dye, which can
51 enter into intact mitochondria selectively [44]. While after 24 h exposure to 10 μM PF1022A
52 a moderate mitochondrial membrane depolarisation was shown (12.4% of cells vs. 4.3% in
53
54
55
56
57
58
59
60
61
62
63
64
65

1 control) this effect was distinctly enhanced after 48 h treatment (32% of cells vs. control of
2 3%) (Fig.4C). In contrast, PF1022A did not affect the mitochondrial membrane potential at
3
4 concentrations $\leq 2.5 \mu\text{M}$, independent of exposure time (data not shown).
5
6
7
8

9 **3.7. Impact of PF1022A on cell cycle distribution**

10 To further investigate whether PF1022A affect the cell cycle distribution flow cytometric
11 analyses were performed in KB-3-1 cells and histograms were gated on live cells. PF1022A
12 treatment caused a moderate concentration-dependent increase in the number of cells in
13
14 G_0/G_1 -phase after 24 h and 48 h (Fig. 4). This effect was distinct at concentrations $\geq 5 \mu\text{M}$ as
15
16 shown by an increase of cells in G_0/G_1 -phase by 23% and 19% after 24- and 48 h exposure,
17
18 respectively. Additionally, after 24- and 48 h treatment with $10 \mu\text{M}$ PF1022A a further
19
20 increase was observed by 43% and 34%, respectively. In accordance, the number of cells in
21
22 the S- and G_2/M -phase significantly decreased at these concentrations
23
24
25
26
27
28
29
30
31
32
33

34 **3.8. Impact of apoptosis- and cell cycle-regulating proteins p53, p21, Bax, and Bcl-2 on** 35 **PF1022A-induced cell death.**

36 To further investigate the mechanisms underlying PF1022A-induced cell death, the effect of
37
38 apoptosis- and cell cycle regulating proteins was studied. For this purpose, HCT116 cells with
39
40 disrupted p53, p21 or bax genes as well as A549 cells with stably overexpressing bcl-2 gene
41
42 (A549/Bcl-2) were used. In general, in all tested cell lines a distinct cytotoxic effect was
43
44 observed at high concentrations ($10 \mu\text{M}$). Remarkably, deletion of p53 was accompanied with
45
46 loss of sensitivity to high PF1022A concentrations (Tab. 1). Comparable effects were
47
48 observed in HCT116 bax (-/-) cells (Tab. 1). In contrast, the cytotoxic effect of PF1022A was
49
50 more prominent in HCT116 p21 (-/-) cells than in the respective parental cell clone (Tab. 1).
51
52
53
54
55
56
57
58
59
60
61
62
63
64
65

Effects of PF1022A on cell growth of A549 with transfected Bcl2 and the A549 vector control did not differ significantly from each other.

4. Discussion

The anthelmintic drug PF1022A is active against diverse worms when administered orally or parenterally. Depending on the species of worms and the host, helminths are paralysed in concentrations ranging from 1 to 10 mg/kg body weight [8, 26], which coincides with the *in vitro* activity at 1 µg/ml against *Trichinella spiralis* and *Nippostrongylus brasiliensis* [45] as well as the effect at 1 µM PF1022A against *Haemonchus contortus* [6]. The lack of an effect on f_c at 1 µM and an estimated IC_{50} of 25 µM for isolated guinea-pig ileum demonstrate that contractility is not reduced significantly at anthelmintic active concentrations. Consequently, the peristalsis which is necessary to transfer food through the gut should not be affected by the drug. Comparable to other cyclohexadepsipeptides [46, 47], PF1022A influenced the intracellular Ca^{2+} concentration in Caco-2 cells only at high drug concentrations (≥ 30 µM). Sustained Ca^{2+} elevation usually results in dysfunction of the contractile mechanism, which might be the cause of the observed reduction in the force of contraction in isolated guinea pig ileum at high drug concentrations.

Results obtained from electrophysiological experiments give evidence that the cyclooctadepsipeptide PF1022A interacts with mammalian cells. The drug was shown to incorporate into cell membranes forming cation selective channels, similar to the cyclohexadepsipeptides beauvericin [48] and enniatin [40]. Patch clamp studies revealed that PF1022A manifests common traits of physiological ion channel behaviour such as unitary transitions in conductance levels characteristic for channels, selectivity, rectification, and

1
2
3
4
5
6
7
8
9
10
11
12
13
14
15
16
17
18
19
20
21
22
23
24
25
26
27
28
29
30
31
32
33
conductances in the pS range. This strongly suggests that PF1022A is a potential channel-
forming ionophore. Moreover, formation of a sandwich complex can be postulated similar to
the cyclohexadepsipeptides beauvericin [49] and enniatin [50]. Through such PF1022A-
induced membrane spanning pores, ions are able to diffuse at both directions following their
electrochemical gradient. This conformation would allow the symmetry depicted in the
current-voltage curves and the sort of electrostatic interaction that prevailed in our
experiments, making the pore selective to cations. However, contrary to beauvericin and
enniatin, the kinetics of the PF1022A-induced channel were not influenced by conducted
cations. Although this ionophoric action was found already at very low drug concentrations,
ion influx affected intracellular ion concentrations only minimally, even at high drug
concentrations. Thus, these changes in intracellular ion concentrations might not contribute
markedly to cellular toxicity. Apart from these findings, it has been already demonstrated that
the ionophoric activity does not correlate with the anthelmintic potency of
cyclooctadepsipeptides [28].

34
35
36
37
38
39
40
Besides the ionophoric activity, electrophysiological effects via modulation of the GABA
current are discussed, as in binding studies it could be demonstrated that PF1022A binds to
GABA receptors in nematodes, probably contributing to the anthelmintic effect [27].

41
42
43
44
45
46
47
48
49
50
51
52
53
54
55
56
57
58
59
60
61
62
63
64
65
Therefore, we tested whether PF1022A exerts any effect on GABA_A receptors composed of
 $\alpha 1$, $\beta 2$ and $\gamma 2S$ subunits, which might be of interest in terms of sedative side effects during
anthelmintic therapy. Significant activation of the GABA current, however, was not observed.
For the reason of diverse pharmacological properties of structurally related compounds, and
in order to prove low cellular toxicity of PF1022A at anthelmintic concentrations, a panel of
cytotoxicity tests was performed in mammalian cells. Cytotoxic effects after different
exposure times to PF1022A occurred at micromolar concentrations but higher than the active
anthelmintic concentrations. Since the results obtained in experiments with and without

1 washout phase did not differ significantly at PF1022A concentrations $> 5\mu\text{M}$ and only a small
2 number of cells could recover, a potent cytotoxic effect of this cyclooctadepsipeptide was
3 suggested at high concentrations. In contrast, at low anthelmintic concentrations ($0.5\text{-}1\ \mu\text{M}$)
4 PF1022A significantly enhanced proliferation of the tumour cell line KB-3-1. Comparable
5 effects were reported for the structurally related enniatins [31]. This growth stimulating
6 activity was suggested to be based on compensatory mechanisms to enniatins-induced stress
7 signals [31].

8
9
10
11
12
13
14
15
16 Regarding PF1022A-induced cytotoxicity, apoptosis induction via the mitochondrial pathway
17 was suggested at least for long-term PF1022A treatment at high concentrations. This was
18 based on a significant depolarisation of the mitochondrial membrane potential, which is an
19 important step to trigger programmed cell death, after 48 h PF1022A treatment with $10\ \mu\text{M}$
20 [50]. Moreover, several characteristics of programmed cell death like cell shrinkage,
21 chromatin condensation and apoptotic body formations were observed after 48 h drug
22 treatment with $10\ \mu\text{M}$ PF1022A. Furthermore, the complete lack of cellular lactate
23 dehydrogenase release indicative for necrotic cell death emphasizes the apoptotic activity of
24 the anthelmintic drug. These results are comparable to the cytotoxic effects of the
25 structurally related cyclohexadepsipeptides enniatins [31] and beauvericin [32, 33]. Moreover,
26 since the ionophoric activity of these cyclic peptides was suggested to contribute to their
27 potent cytotoxicity [33, 46, 53], comparable modes of actions might be hypothesized for
28 PF1022A. However, our study revealed that only high concentrations ($100\ \mu\text{M}$) of the
29 cyclooctadepsipeptide PF1022A cause an increase in the intracellular Ca^{2+} levels. Thus, this
30 effect does not seem to contribute markedly to cytotoxicity.

31
32
33
34
35
36
37
38
39
40
41
42
43
44
45
46
47
48
49
50
51
52
53 In addition to apoptosis induction, our study revealed that long-term but also short-term
54 PF1022A treatment concentration-dependently led to cell cycle arrest in G_0/G_1 phase. Thus,
55 the cytotoxic modes of actions of short-term PF1022A exposure might be based on a cell
56
57
58
59
60
61
62
63
64
65

1 cycle blockade. Consistently, data obtained by DAPI staining revealed a significant reduction
2 of countable nuclei compared to control after 24 h drug treatment. Moreover, cells with
3 deleted cyclin-dependent kinase inhibitor p21 were more sensitive to PF1022A-induced
4 cytotoxicity. This suggests that cell cycle blockade via p21 might rescue cells from PF1022A-
5 induced cell death as it was also suggested for the structurally related enniatins [31].
6

7
8
9
10
11 To further investigate the impact of PF1022A on apoptosis- and cell cycle-regulating proteins,
12 HCT116 cells with disrupted p53, p21 or bax genes [37, 38, 39] and A549 cells transfected
13 with Bcl-2 were used. In MTT assays, a small shift of cytotoxicity to higher PF1022A
14 concentrations was observed in p53 and bax disrupted cells, whereas the apoptosis inhibitor
15 Bcl-2 had no significant influence on PF1022A-induced cell death. Thus, our data suggest
16 that PF1022A-induced mitochondrial membrane depolarisation occurs via a molecular
17 mechanism involving p53-mediated apoptosis effects. This is in contrast to enniatins, which
18 mediated apoptosis induction independent of either of these proteins, but activated the
19 proapoptotic p53-downstream target bax at relatively low enniatin concentrations [31].
20
21

22
23
24
25
26
27
28
29
30
31
32
33 To conclude, data obtained with PF1022A in mammalian tissue and cells point to drug safety
34 in terms of lower susceptibility of mammalian tissue compared to the paralysing effect in
35 helminths. Moreover, due to the lack of an effect on $I_{GABA(A)}$ at anthelmintic concentrations no
36 sedative side effects are to be expected. In addition, the drug PF1022A and its derivatives
37 might be of interest to be studied in more detail in respect to anticancer activity.
38
39
40
41
42
43
44
45
46
47
48
49
50
51
52
53
54
55
56
57
58
59
60
61
62
63
64
65

5. References

- 1
2
3
4
5 [1] Bundy DA, de Silva NR. Can we deworm this wormy world? *Br Med Bull* 1998;54:421-
6
7 32.
8
9
10 [2] Waller PJ. Anthelmintic resistance. *Vet Parasitol* 1997;72:391-412.
11
12 [3] von Samson-Himmelstjerna G, Harder A, Sangster NC, Coles GC. Efficacy of two
13 cyclooctadepsipeptides, PF1022A and emodepsidde, against anthelmintic-resistant
14 nematodes in sheep and cattle. *Parasitology* 2005;130:343-7.
15
16
17 [4] Geary TG, Sangster NC, Thompson DP. Frontiers in anthelmintic pharmacology. *Vet*
18
19
20
21
22
23
24
25 [5] Sasaki T, Takagi M, Yaguchi T, Miyadoh S, Okada T, Koyama M. A new anthelmintic
26
27
28
29
30
31
32
33
34
35
36
37 [6] Conder GA, Johnson SS, Nowakovski DS, Blake TE, Dutton FE, Nelson SJ, et al.
38
39
40
41
42
43
44
45
46
47
48
49
50
51
52
53
54
55
56
57
58
59
60
61
62
63
64
65
- [7] Kachi S, Terada M, Hashimoto H. Effect of PF1022A on adult *Angiostrongylus*
cantonensis in the pulmonary arteries and larvae migrating into the central nervous system
in rats. *Parasitol Res* 1995; 81:631-7.
- [8] von Samson-Himmelstjerna G, Harder A, Schmieder T, Kalbe J, Mencke N. In vivo
activities of the new anthelmintic depsipeptide PF1022A. *Parasitol Res* 2000;86:194-9.
- [9] Zahner H, Taubert A, Harder A, von Samson-Himmelstjerna G. Filaricidal efficacy of
anthelmintically active cyclodepsipeptides. *Int J Parasitol* 2001;31:1515-2.
- [10] Mentz MB, Graeff-Teixeira C. Drug trials for treatment of human angiostrongyliasis. *Rev*
Inst Med trop S Paulo 2003;45:179-4.

- 1
2
3
4
5
6
7
8
9
10
11
12
13
14
15
16
17
18
19
20
21
22
23
24
25
26
27
28
29
30
31
32
33
34
35
36
37
38
39
40
41
42
43
44
45
46
47
48
49
50
51
52
53
54
55
56
57
58
59
60
61
62
63
64
65
- [11] Weckwerth W, Miyamoto K, Iinuma K, Krause M, Glinski M, Storm T, et al. Biosynthesis of PF1022A and related cyclooctadepsipeptides. *J Biol Chem* 2000;275:17909-15.
- [12] Krause M. Untersuchungen zur Biosynthese des Cyclooctadepsipeptids PF1022A. Dissertation TU Berlin 1998.
- [13] Yanai K, Sumida N, Okakura K, Moriya T, Watanabe M, Murakami T. Para-position derivatives of fungal anthelmintic cyclodepsipeptides engineered with *Streptomyces venezuelae* antibiotic biosynthetic genes. *Nat Biotechnol* 2004;22:848-5.
- [14] Jeschke P, Iinuma K, Harder A, Schindler M, Murakami T. Influence of the cyclooctadepsipeptide PF1022A and PF1022E as natural products on the design of the semi-synthetic anthelmintics such as emodepside. *Parasitol Res* 2005;97:511-6.
- [15] Jeschke P, Harder A, Etzel W, Gau W, Thielking G, Bonse G, et al. Synthesis and anthelmintic activity of thioamide analogues of cyclic octadepsipeptides such as PF1022A. *Pest Manag Sci* 2001;57:1000-6.
- [16] Jeschke P, Harder A, von Samson-Himmelstjerna G, Etzel W, Gau W, Thielking G, et al. Synthesis of anthelmintically active N-methylated amidoxime analogues of the cyclic octadepsipeptide PF1022A. *Pest Manag Sci* 2002;58:1205-15.
- [17] Dyker H, Harder A, Scherkenbeck J. Chimeric cyclodepsipeptides as mimetics for the anthelmintic PF1022A. *Bioorg Med Chem Lett* 2004;14:6129-2.
- [18] Dutton FE, Nelson SJ. Synthesis of PF1022A, an anthelmintic cyclodepsipeptide. *J Antibiot (Tokyo)* 1994;47:1322-7.
- [19] Dutton FE, Lee BH, Johnson SS, Coscarelli EM, Lee PH. Restricted conformation analogues of an anthelmintic cyclodepsipeptide. *J Med Chem* 2003;46:2057-73.

- 1
2
3
4
5
6
7
8
9
10
11
12
13
14
15
16
17
18
19
20
21
22
23
24
25
26
27
28
29
30
31
32
33
34
35
36
37
38
39
40
41
42
43
44
45
46
47
48
49
50
51
52
53
54
55
56
57
58
59
60
61
62
63
64
65
- [20] Lee BH, Dutton FE, Thompson DP, Thomas EM. Generation of a small library of cyclodepsipeptide PF1022A analogues using a cyclization-cleavage method with oxime resin. *Bioorg Med Chem Lett* 2002;12:353-6.
- [21] Scherkenbeck J, Jeschke P, Harder A. PF1022A and related cyclodepsipeptides – a novel class of anthelmintics. *Curr Top Med Chem* 2002;2:759-77.
- [22] Scherkenbeck J, Harder A, Plant A, Dyker H. PF1022A – a novel anthelmintic cyclooctadepsipeptide. Modification and exchange of the N-methyl leucine residues. *Bioorg Med Chem Lett* 1998;8:1035-0.
- [23] Saeger B, Schmitt-Wrede HP, Dehnhardt M, Benten WPM, Krücken J, Harder A, v Samson-Himmelstjerna G, Wiegand H, Wunderlich F. Latrophilin-like receptor from the parasitic nematode *Haemonchus contortus* as target for the anthelmintic depsipeptide PF1022A. *FASEB J* 2001;15:1332-54
- [24] Harder A, Schmitt-Wrede, Krücken J, Marinovski P, Wunderlich F, Willson J, et al. Cyclooctadepsipeptides – an anthelmintically active class of compounds exhibiting a novel mode of action. *Int J Antimicrob Agents* 2003;22:318-31.
- [25] Harder A, Holden-Dye L, Walker R, Wunderlich F. Mechanisms of action of emodepside. *Parasitol Res* 2005;97:S1-S10.
- [26] Harder A, von Samson-Himmelstjerna G. Cyclooctadepsipeptides – a new class of anthelmintically active compounds. *Parasitol Res* 2002;88:481-8.
- [27] Chen W, Terada M, Cheng JT. Characterization of subtypes of gamma-aminobutyric acid receptors in an *Ascaris* muscle preparation by binding assay and binding of PF1022A, a new anthelmintic, on the receptor. *Parasitol Res* 1996;82:97-101.
- [28] Gessner G, Meder S, Rink T, Boheim G, Harder A, Jeschke P, et al. Ionophore and anthelmintic activity of PF1022A, a cyclooctadepsipeptide, are not related. *Pestic Sci* 1996;48:399-407.

- 1
2
3
4
5
6
7
8
9
10
11
12
13
14
15
16
17
18
19
20
21
22
23
24
25
26
27
28
29
30
31
32
33
34
35
36
37
38
39
40
41
42
43
44
45
46
47
48
49
50
51
52
53
54
55
56
57
58
59
60
61
62
63
64
65
- [29] Zhang L, Yan K, Zhang Y, Huang R, Bian J, Zheng C, et al. High-throughput synergy screening identifies microbial metabolites as combination agents for the treatment of fungal infections. *Proc Natl Acad Sci* 2007;104:4606-11.
- [30] Fukuda T, Arai M, Yamaguchi Y, Masuma R, Tomoda H, Omura S. New beauvericins, potentiators of antifungal miconazole activity, produced by *Beauveria* sp. FKI-1366. Taxonomy, fermentation, isolation and biological properties. *J Antibiot* 2004;57:110-6.
- [31] Dornetshuber R, Heffeter P, Kamyar M, Peterbauer T, Berger W, Lemmens-Gruber R. Enniatin induces apoptosis and exerts p53-dependent cytostatic and p53-independent cytotoxic activities against human cancer cells. *Chem Res Toxicol* 2007;20:465-73.
- [32] Lin HI, Lee YJ, Chen BF, Tsai MC, Lu JL, Chou CJ, et al. Involvement of Bcl-family, cytochrome c and caspase 3 in induction of apoptosis by beauvericin in human non-small cell lung cancer cells. *Cancer Lett* 2005;239:248-59.
- [33] Jow GM, Chou CJ, Chen BF, Tsai JH. Beauvericin induces cytotoxic effects in human acute lymphoblastic leukemia cells through cytochrome c release, caspase 3 activation: the causative role of calcium. *Cancer Lett* 2004;216:165-73.
- [34] Zhan J, Burns AM, Liu MX, Faeth SH, Gunatilaka AAL. Search for cell motility and angiogenesis inhibitors with potential anticancer activity: beauvericin and other constituents of two endophytic strains of *Fusarium oxysporum*. *J Nat Prod* 2007;70:227-32.
- [35] Jeschke P, Benet-Buchholz J, Harder A, Etzel W, Schindler M, Gau W, et al. Synthesis and anthelmintic activity of substituted (R)-phenyllactic acid containing cyclohexadepsipeptides. *Bioorg Med Chem Lett* 2006;16:4410-5.
- [36] Shen DW, Cardarelli C, Hwang J, Cornwell M, Richert N, Ishii S, Pastan I, Gottesman MM (1986). Multiple drug-resistant human KB carcinoma cells independently selected

- 1
2
3
4
5
6
7
8
9
10
11
12
13
14
15
16
17
18
19
20
21
22
23
24
25
26
27
28
29
30
31
32
33
34
35
36
37
38
39
40
41
42
43
44
45
46
47
48
49
50
51
52
53
54
55
56
57
58
59
60
61
62
63
64
65
- for high-level resistance to colchicine, adriamycin, or vinblastine show changes in expression of specific proteins. *J Biol Chem* 1986;261:7762-70.
- [37] Bunz F, Fauth C, Speicher MR, Dutriaux A, Sedivy JM, Kinzler KW, et al. Targeted inactivation of p53 in human cells does not result in aneuploidy. *Cancer Res* 2002;62:1129-33.
- [38] Waldman T, Kinzler KW, Vogelstein B. p21 is necessary for the p53-mediated G1 arrest in human cancer cells. *Cancer Res* 1995;55:5187-90.
- [39] Zhang L, Yu J, Park BH, Kinzler KW, Vogelstein B. Role of BAX in the apoptotic response to anticancer agents. *Science* 2000;290:989-92.
- [40] Kamyar MR, Rawnduzi P, Studenik C, Kouri K, Lemmens-Gruber R. Investigation of the electrophysiological properties of enniatin. *Arch Biochem Biophys* 2004;429:215-23.
- [41] Khom S, Baburin I, Timin EN, Hohaus A, Sieghart W, Hering S. Pharmacological properties of GABA_A receptors containing gamma1 subunits. *Mol Pharmacol* 2006;69:640-9.
- [42] Methfessel C, Witzemann V, Takahashi T, Mishina M, Numa S, Sakmann B. Patch clamp measurements on *Xenopus laevis* oocytes: currents through endogenous channels and implanted acetylcholine receptor and sodium channels. *Pflugers Arch* 1986;407:577-88.
- [43] Baburin I, Beyl S, Hering S. Automated fast perfusion of *Xenopus* oocytes for drug screening. *Pflugers Arch* 2006;453: 117-23.
- [44] Heffeter P, Jakupec MA, Körner W, Chiba P, Pirker C, Dornetshuber R, Elbling L, Sutterlüty H, Micksche M, Keppler BK, Berger W. Multidrug-resistant cancer cells are preferential targets of the new antineoplastic lanthanum compound KP772 (FFC24). *Biochem Pharmacol* 2007;73:1873-86.

- 1
2
3
4
5
6
7
8
9
10
11
12
13
14
15
16
17
18
19
20
21
22
23
24
25
26
27
28
29
30
31
32
33
34
35
36
37
38
39
40
41
42
43
44
45
46
47
48
49
50
51
52
53
54
55
56
57
58
59
60
61
62
63
64
65
- [45] Martin RJ, Harder A, Londerhausen M, Jeschke P. Anthelmintic actions of the cyclic depsipeptide PF1022A and its electrophysiological effects on muscle cells of *Ascaris suum*. *Pest Sci* 1996;48:343-9.
- [46] Kouri K, Duchen MR, Lemmens-Gruber R. Effects of beauvericin on the metabolic state and ionic homeostasis of ventricular myocytes of the guinea pig. *Chem Res Toxicol* 2005;18:1661-8.
- [47] Kamyar MR, Kouri K, Rawnduzi P, Studenik C, Lemmens-Gruber R. Effects of moniliformin in presence of cyclohexadepsipeptides on isolated mammalian tissue and cells. *Toxicol In Vitro* 2006;20:1284-91.
- [48] Kouri K, Lemmens M, Lemmens-Gruber R. Beauvericin induced channels in ventricular myocytes and artificial membranes. *Biochim Biophys Acta* 2003;1609:203-10.
- [49] Ivanov VT, Evstratov AV, Sums kaya LV, Melnik EI, Chumburidze TS, Portnova SL, Balashova TA, Ovchinnikov YA. Sandwich complexes as a functional form of the enniatin ionophores. *FEBS Letters* 1973;36:65-71.
- [50] Ovchinnikov YA, Ivanov VT, Evstratov AV, Mikhaleva II, Bystrov VF, Portnova SL, Balashova TA, Meshcheryakova EN, Tulchinsky VM. The enniatin ionophores. Conformation and ion binding properties. *Int J Peptide Protein Res* 1974;6:465-498
- [51] Fadeel B, Orrenius S. Apoptosis: a basic biological phenomenon with wide-ranging implications in human disease. *J Int Med* 2005;258:479-517.
- [52] Los M, Mozoluk M, Ferrari D, Stepczynska A, Stroh C, Renz A, et al. Activation and caspase-mediated inhibition of PARP: a molecular switch between fibroblast necrosis and apoptosis in death receptor signalling. *Mol Biol Cell* 2002;13:978-88.
- [53] Tang Y, Chen YW, Jow GM, Chou CJ, Jeng CJ. Beauvericin activates Ca^{2+} -activated Cl^- currents and induces cell deaths in *Xenopus* oocytes via influx of extracellular Ca^{2+} . *Chem Res Toxicol* 2005;18:825-33.

Figure legends:

1
2
3
4
5 **Fig. 1:** Pore-forming activity and changes in intracellular ion concentrations. In (A) typical
6 recordings of a Ca^{2+} current from an inside-out patch are shown. The dashed line marks the
7 closed state “c”; downward deflections indicate channel openings. The holding potential was
8 held at -60 mV. The upper trace 1 shows a control recording without openings. Traces 2 and
9 3 represent single and multiple channel openings in presence of 1 and 10 μM PF1022A,
10 respectively. The small increase in intracellular Ca^{2+} concentration (expressed as ratio
11 $F_{340\text{nm}}/F_{380\text{nm}}$) caused by 100 μM PF1022A (C) is shown for three representative cells in
12 comparison to 100 μM ionomycin (B) (note the difference in scale on the ordinate). At 10 μM
13 no changes in $[\text{Ca}^{2+}]_i$ were observed (data not shown). The effect on intracellular K^+
14 concentration is shown for 100 μM PF1022A (E) and 100 μM valinomycin (D) for two
15 representative cells each.
16
17
18
19
20
21
22
23
24
25
26
27
28
29
30

31
32
33
34 **Fig. 2:** Concentration-dependent effect on cell growth is demonstrated in KB-3-1 cells after
35 exposure to PF1022A for 24, 48 h and 72h. After the respective treatment durations, drug
36 solution was replaced by 100 μl MTT solution and viability was measured by a microplate
37 reader, set at 450 nm with 620 nm as reference to reduce unspecific background values. All
38 experiments were performed at least twice in triplicates. ^(a) Cell growth-stimulating and ^(b)
39 cytotoxic effects were significantly (*, **, ***: $P < 0.05$, < 0.01 , < 0.001 , respectively)
40 different to untreated control (Student’s t-test).
41
42
43
44
45
46
47
48
49
50

51
52
53
54 **Fig. 3:** (A, B) Nuclei of KB-3-1 cells were stained with DAPI, classified (in interphase,
55 mitotic, and apoptotic) and counted. Means \pm SD were calculated from at least 500 nuclei
56 from three independent experiments. *, **, significant ($P < 0.05$, < 0.01 , respectively)
57
58
59
60
61
62
63
64
65

1 difference between PF1022A-treated and -untreated cells was calculated using the Student's t-
2 test. (C) Changes in the mitochondrial membrane potential were measured after 24 h and 48 h
3 of PF1022A treatment using the fluorescent dye JC-1. Percentages of apoptotic (green
4 fluorescent, FL-1) cells, located in the right lower quarter, are indicated at the left bottom.
5
6
7
8
9

10
11 **Fig. 4** PI staining and FACS analyses were performed on KB-3-1 cells after 24 h and 48 h
12 PF1022A exposure at the indicated drug concentrations. Percentages of cells in the G₀/G₁, S,
13 and G₂/M phases of the cell cycle as well as apoptotic cells are indicated. *, **, significantly
14 (P < 0.05, < 0.01, respectively) different to untreated cells (Student's t-test).
15
16
17
18
19
20
21
22
23
24
25
26
27
28
29
30
31
32
33
34
35
36
37
38
39
40
41
42
43
44
45
46
47
48
49
50
51
52
53
54
55
56
57
58
59
60
61
62
63
64
65

Fig. 1

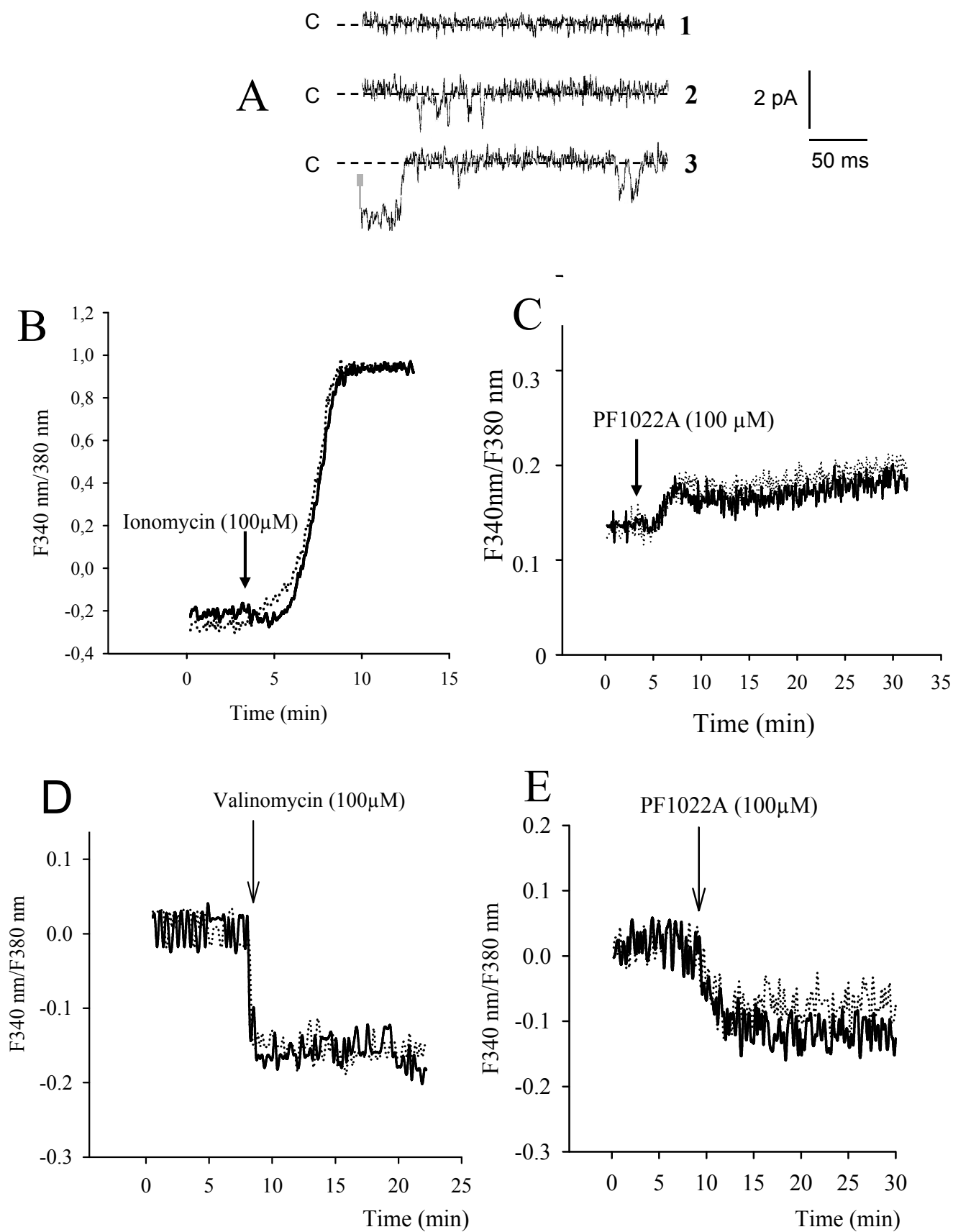


Fig. 2

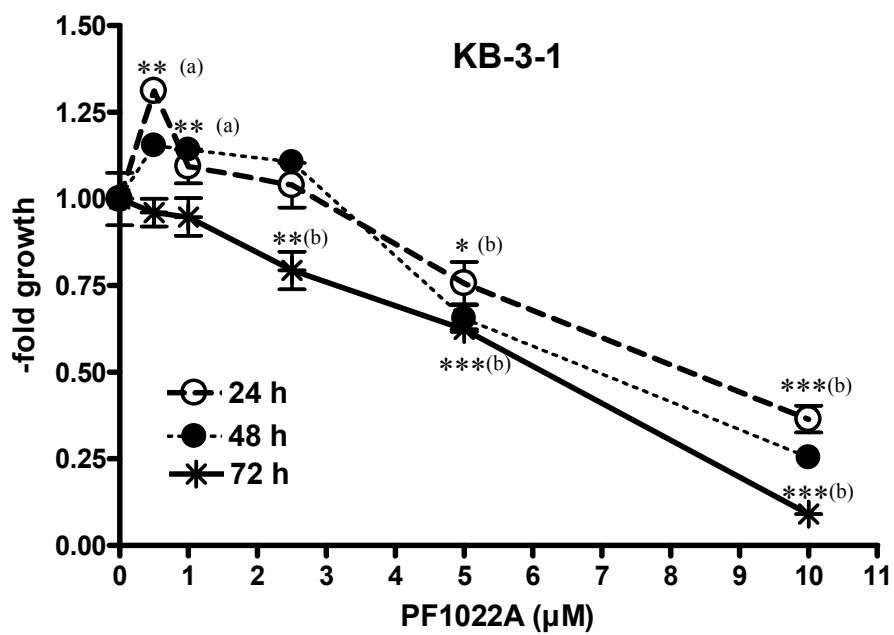


Fig. 3

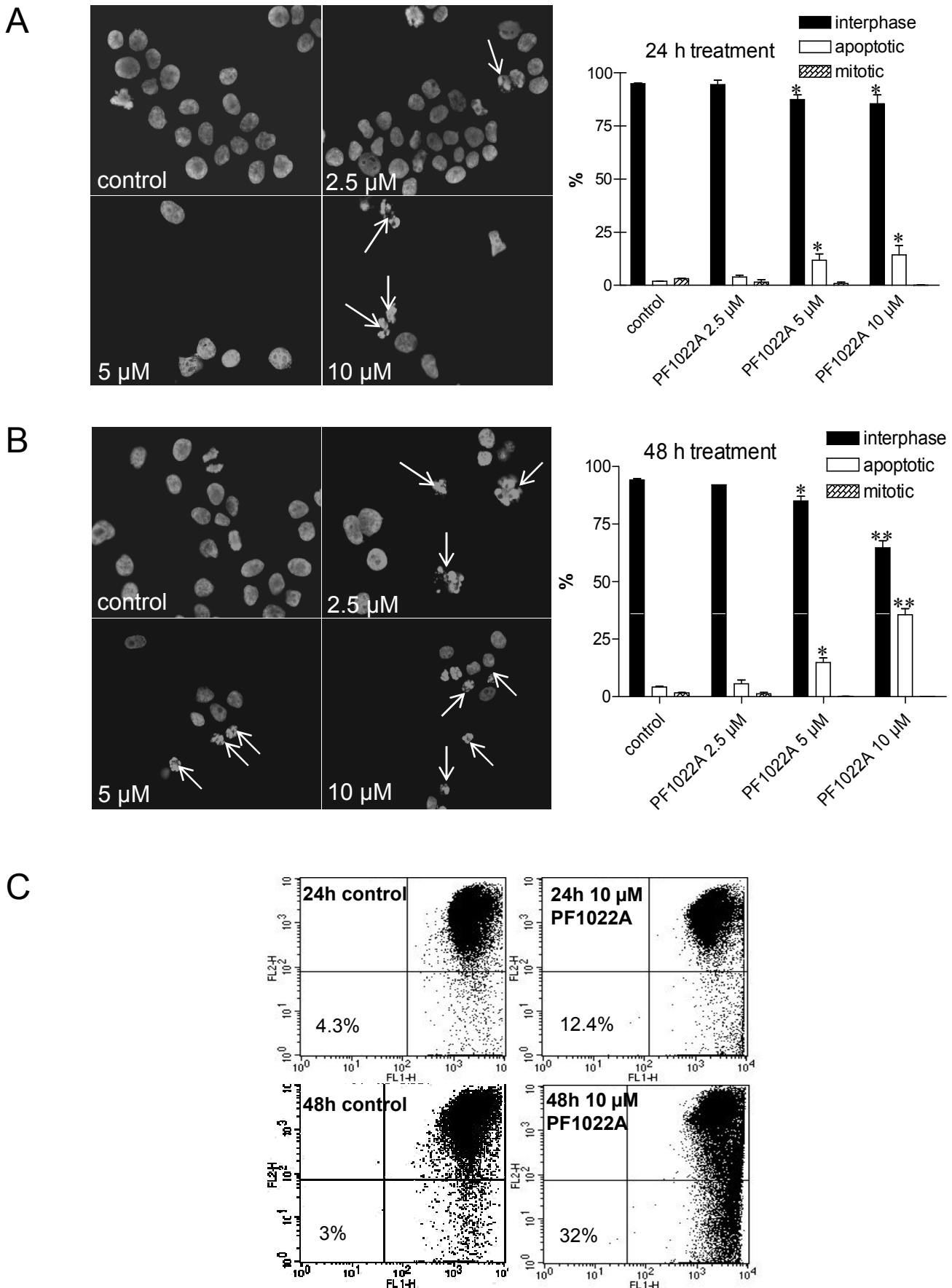


Fig. 4

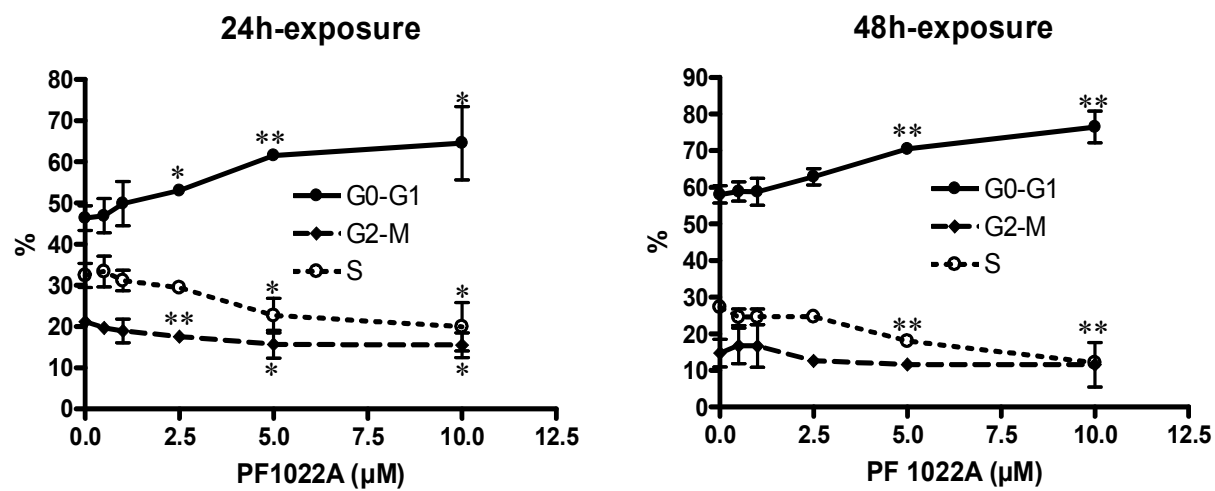


Table 1: Impact of apoptosis- and cell cycle-regulating proteins p53, p21, Bax, and Bcl-2 on PF1022A-induced cell death. IC₅₀ values (μ M) for the time-dependent cytotoxic effect of PF1022A are given.

Cell line	48 h	72 h
HCT 116 p53 (+/+)	8.4 \pm 0.1	7.5 \pm 0.1
HCT 116 p53 (-/-)	9.6 \pm 0.3	9.1 \pm 0.1
HCT 116 bax (+/+)	7.4 \pm 0.3	7.1 \pm 0.1
HCT 116 bax (-/-)	9.5 \pm 0.1	8.2 \pm 0.1
HCT 116 p21 (+/+)	9.4 \pm 0.1	8.2 \pm 0.1
HCT 116 p21 (-/-)	6.0 \pm 0.1	4.6 \pm 0.1
A549/Bcl-2	7.5 \pm 0.1	4.3 \pm 0.2
A549/vc	7.3 \pm 0.1	4.6 \pm 0.1

Cytotoxicity of the ionophoric cyclooctadepsipeptide PF1022A is induced by apoptosis via the mitochondrial pathway and cell cycle blockade in G₀/G₁ phase at concentrations higher than those used in anthelmintic treatment.

